

# Modeling vacancies and hydrogen impurities in graphene: A molecular point of view

G. Forte<sup>a</sup> A. Grassi<sup>a</sup> G. M. Lombardo<sup>a</sup> A. La Magna<sup>b</sup>  
G. G. N. Angilella<sup>c,d,e,1</sup> R. Pucci<sup>c,e</sup> R. Vilardi<sup>c</sup>

<sup>a</sup>*Dipartimento di Scienze Chimiche, Facoltà di Farmacia, Università di Catania,  
Viale A. Doria, 6, I-95126 Catania, Italy*

<sup>b</sup>*IMM, CNR, Catania, Italy*

<sup>c</sup>*Dipartimento di Fisica e Astronomia, Università di Catania,  
Via S. Sofia, 64, I-95123 Catania, Italy*

<sup>d</sup>*INFN, Sez. Catania, Italy*

<sup>e</sup>*CNISM, UdR di Catania, Italy*

---

## Abstract

We have followed a ‘molecular’ approach to study impurity effects in graphene. This is thought as the limiting case of an infinitely large cluster of benzene rings. Therefore, we study several carbon clusters, with increasing size, from phenalene, including three benzene rings, up to coronene 61, with 61 benzene rings. The impurities considered were a chemisorbed H atom, a vacancy, and a substitutional proton. We performed HF and UHF calculations using the STO-3G basis set. With increasing cluster size in the absence of impurities, we find a decreasing energy gap, here defined as the HOMO-LUMO difference. In the case of H chemisorption or a vacancy, the gap does not decrease appreciably, whereas it is substantially reduced in the case of a substitutional proton. The presence of an impurity invariably induces an increase of the density of states near the HOMO level. We find a zero mode only in the case of a substitutional proton. In agreement with experiments, we find that both the chemisorbed H, the substitutional proton, and the C atom near a vacancy acquire a magnetic moment. The relevance of graphene clusters for the design of novel electronic devices is also discussed.

PACS: 36.40.Cg, 73.22.-f, 73.20.Hb

---

<sup>1</sup> Corresponding author. E-mail: [giuseppe.angilella@ct.infn.it](mailto:giuseppe.angilella@ct.infn.it).

## 1 Introduction

Since the pioneering works of Wallace [1], Coulson [2], and Semenoff [3], several authors have studied the peculiar electronic and structural properties of graphene, a single sheet of graphite, originally only considered as a prototype of the graphite's surface. A breakthrough in these studies arrived with the experimental realization of graphene [4]. The increasing interest in this material stems both from the analogy of its behavior with many phenomena of quantum electrodynamics (QED) [5], and because of its prospective applications in the fabrication of novel electronic devices. To this aim, it is important to have systems with a tunable band gap. We will stress that the graphene clusters (GC) here considered, even if they are characterized by a zig-zag boundary, have a semiconducting behavior, at variance with zig-zag graphene nanoribbons (ZGNR), which have a metallic behavior [6]. The gap strongly depends on the cluster size, so that it will be highly desirable to have method allowing to control the size of graphene quantum dots.

Graphene is a robust material. However, defects, such as ripples, adatoms, vacancies and charges induced by the substrate, can modify its electronic properties [7]. In the past, the study of vacancies and impurities in carbon-based systems has been important for several aspects.

(i) Graphene nanostructures are believed to be attractive structures for hydrogen storage. Preliminary results in this direction have been reported in the case of single-walled carbon nanotubes (SWCNT) [8].

(ii) It has been found [9] that proton irradiation of highly oriented pyrolytic graphite samples triggers ferro- or ferrimagnetism. It is now commonly accepted that not only vacancies, but also hydrogen chemisorbed on graphene can acquire a magnetic moment.

(iii) From an astrophysical point of view, it would be of interest to understand why  $\text{H}_2$  is the most abundant molecule in the interstellar medium (ISM), despite the continuous dissociation of molecular hydrogen by UV radiation and cosmic rays [10].

Of course, there can be relevant differences in the characterization of defects in graphite, nanotubes, or graphene. For instance, if one considers the screening of a charged impurity, Cheianov and Fal'ko [11] have shown that the electron density  $\delta\rho$  in graphene decays as  $\delta\rho(r) \sim r^{-3}$  at long distances  $r$  from the impurity. Such a behavior should be contrasted with that derived by Lau and Kohn [12] for a two-dimensional (2D) electron gas, where  $\delta\rho(r) \sim r^{-2}$ . The reason of such a difference is due to the peculiar chiral properties of the electrons in graphene. It has been suggested [13] that such a difference can be used to distinguish between monolayer and bilayer graphene in Fourier transformed

scanning tunneling spectroscopy (FTSTS). Actually, impurity induced quantum interferences have been used in scanning tunneling microscopy (STM) [14] to identify experimentally mono- or bilayer graphene. Previously, STM was used [15,16] to study chemisorption of hydrogen on the basal plane of graphite and atomic vacancy formation.

From a theoretical point of view, the effects on the electronic structure of graphene due to the presence of vacancies, local impurities, and substitutional impurities have been studied by Pereira *et al.* [17], by using a tight-binding Hamiltonian with a local potential  $U$ . These authors have found general trends in the low-energy spectrum of graphene connected with localized zero modes, resonances and gaps induced by the above mentioned defects. However, in some cases, it is important to have a more detailed description of the local interaction of the defects with graphene. For this reason, in the present work, we will make recourse to molecular models, which in the past have been used to study the chemisorption of hydrogen on graphite surface [18,19]. According to these calculations, the graphite surface is modeled as a cluster of benzene rings, whose external dangling bonds are saturated by hydrogen atoms. The most frequently used model clusters are polycyclic aromatic hydrocarbons (PAH), and particularly coronene ( $C_{24}H_{12}$ ). More recently, this model cluster has been used by Patchkovskii *et al.* [20] to study the interaction of molecular hydrogen with graphene nanostructures. These authors have performed calculations at the level of second-order Møller-Plesset (MP2) perturbation theory [21].

In the present work, we will use such model clusters to simulate graphene, at the level of *ab initio* Hartree-Fock (HF) and unrestricted *ab initio* Hartree-Fock (UHF) theory. In some cases, also MP2 calculations will be presented, but the main emphasis will be more on the trends obtained by increasing the cluster size, than in the study of correlation effects. Actually, Martin *et al.* [22] have argued that correlation effects are small in graphene. A similar result was found by Siringo [23] in the study of H chemisorbed on graphene [24]. Furthermore, recently the Manchester group has found that the electron energy levels in quantum dots in graphene follow a statistics characteristic of ‘Dirac billiards’, rather than a Poisson distribution, as is expected for an infinite system [25]: therefore, quantization effects are quite important. It is interesting, in this context, to derive these results also within a molecular approach. In the present work, we have used clusters up to 61 benzene rings, and we have considered the cases of a single vacancy, of a chemisorbed H atom, and of a substitutional proton.

The paper is organized as follows. In Sec. 2, we describe the models used. In Sec. 3 we present our results and a comparison thereof with density functional theory (DFT) and other types of calculations. Finally, in Sec. 4 we summarize and draw our conclusions.

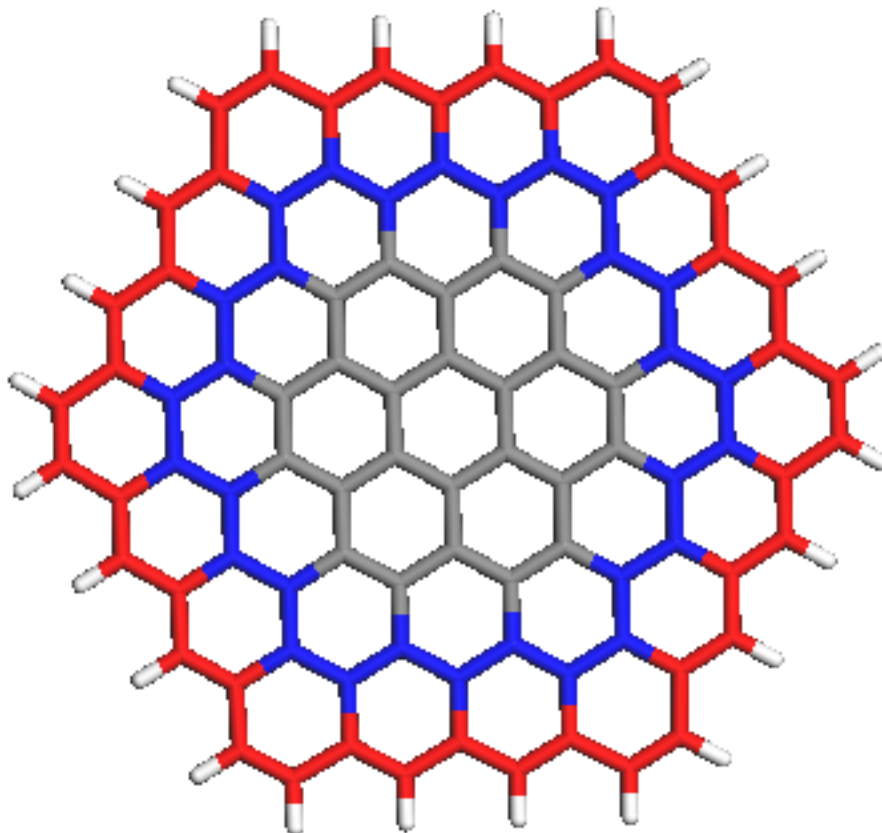


Fig. 1. (Color online.) Showing coronene,  $C_{24}H_{12}$  (gray rods), coronene 19,  $C_{54}H_{18}$  (gray and blue rods), and coronene 37,  $C_{96}H_{24}$  (gray, blue, and red rods).

## 2 The model clusters

The molecular clusters which we have considered are: (i) phenalene (phenalenyl radical); (ii) pyrene; (iii) coronene; (iv) coronene 19, *viz.* coronene surrounded by another series of benzene rings, for a total of 19 benzene rings; (v) coronene 37, *viz.* coronene surrounded by two more series of benzene rings, for a total of 37 benzene rings; (vi) coronene 61. Coronene 37 is shown in Fig. 1. We believe that the larger the cluster, the better it models graphene. For this reason, we have chosen to place in the middle of the cluster: (a) a chemisorbed H atom; (b) a carbon vacancy; (c) a proton in the substitutional position of a carbon atom.

For clusters (i)–(iii) we have used HF calculations with a STO-3G basis set and HF calculations with a 6-311G basis set [26]. In these cases we have also performed MP2 calculations. All the remaining larger clusters have been treated at the HF level using a STO-3G basis set. In the cases of H chemisorption, carbon vacancy and proton substitution, we have performed UHF calculations, because in all these cases there is one  $\pi$ -electron missing. The cluster geometry

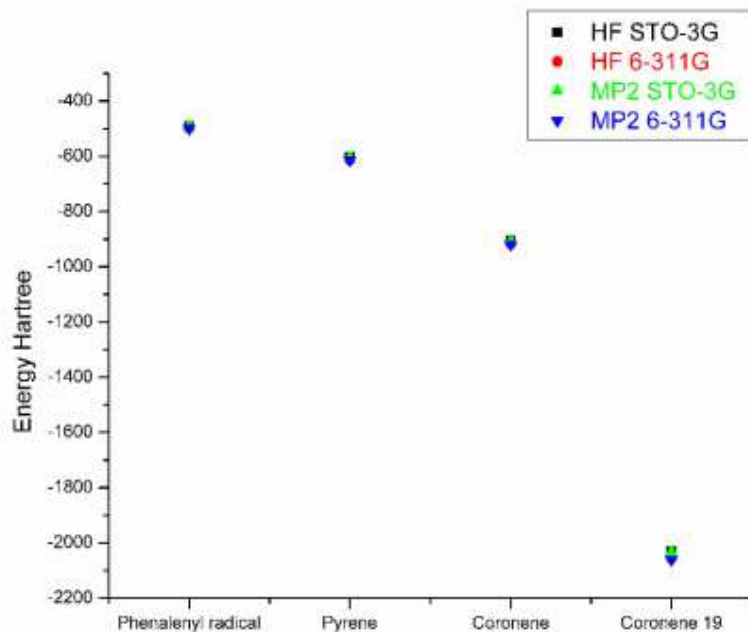


Fig. 2. (Color online.) Showing the dependence of the cluster energy as a function of the cluster under consideration, for the various methods (HF or MP2) and basis sets (STO-3G or 6-311G) employed in the present work. On this scale, the results of different approximations are almost indistinguishable.

has been optimized in all cases.

### 3 Results

#### 3.1 Pure graphene clusters

First of all, we note that the total energy as a function of the number of benzene rings in the clusters (cf. Fig. 2) depends weakly (*i.e.* to within 2 %) on the basis set or on the specific approximation employed (HF, MP2). This lends support to our conviction that relevant conclusions can be drawn already for one of the largest cluster considered, *i.e.* coronene 37, within the framework of the HF approximation with the STO-3G basis set.

Secondly, we note that the gap, which in these kind of calculations is described by the HOMO-LUMO difference, is decreasing by increasing the size of the cluster, as shown in Fig. 3. This is in agreement with the consideration that our clusters resemble more closely graphene, as the number of benzene rings increases. The smallest gap which we have obtained is 5.48 eV.

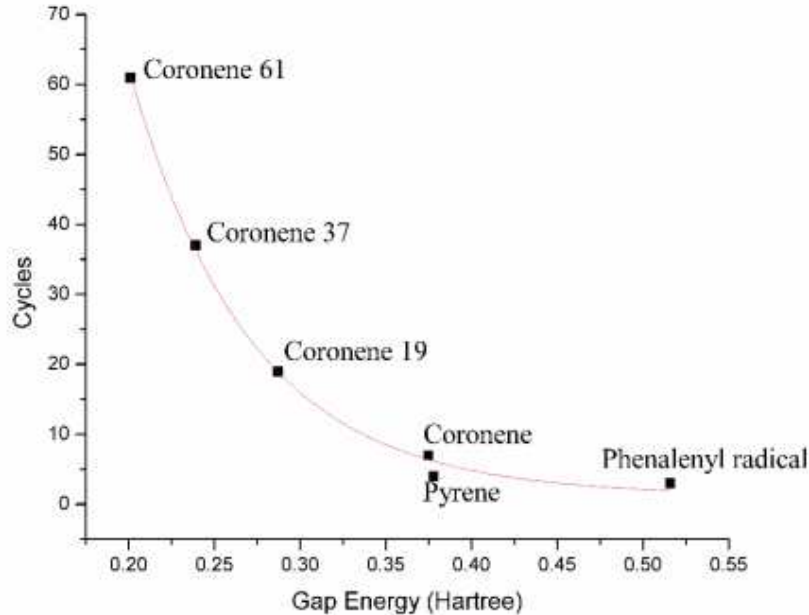


Fig. 3. (Color online.) Showing the dependence of the HOMO-LUMO difference (gap energy) *vs* the number of carbon cycles for the various clusters studied in the present work. The dashed line is a guide to the eye.

Extrapolation of our data seems to indicate that the gap would close at a cluster size of  $\gtrsim 1000$  benzene rings. This is in qualitative agreement with the experimental finding that graphene quantum dots as large as  $\sim 30$  nm are characterized by a gap of  $\sim 0.5$  eV [25]. We find a C-C nearest neighbours equilibrium distance  $d_{C-C} = 1.42$  Å, which is stable with respect to the different approximations and cluster sizes considered here. This is in striking agreement with the typical bond length for  $sp^2$  C-C bonds for graphene and graphite, which is 1.42 Å.

Our minimization procedure yields for the clusters considered in this case a planar configuration, at variance with the experimental finding for graphene, showing the presence of ripples [27,28]. This discrepancy may be related to the specific boundary conditions used in our calculations. Such a result is not in contradiction with the known fact that a nonzero amount of curvature is required in order to stabilize a two-dimensional crystal, as a consequence of Mermin-Wagner theorem [29,30,31]. Indeed, the systems we are considering here are not truly infinite lattices, but rather finite-size clusters. Furthermore, we note that Choi *et al.* [32], by using a cluster with a monovacancy and 127 C atoms, and performing spin-polarized density functional theory calculations, have found an almost planar configuration.

In Fig. 4 we report the density of states (DOS) as a function of energy (eV)

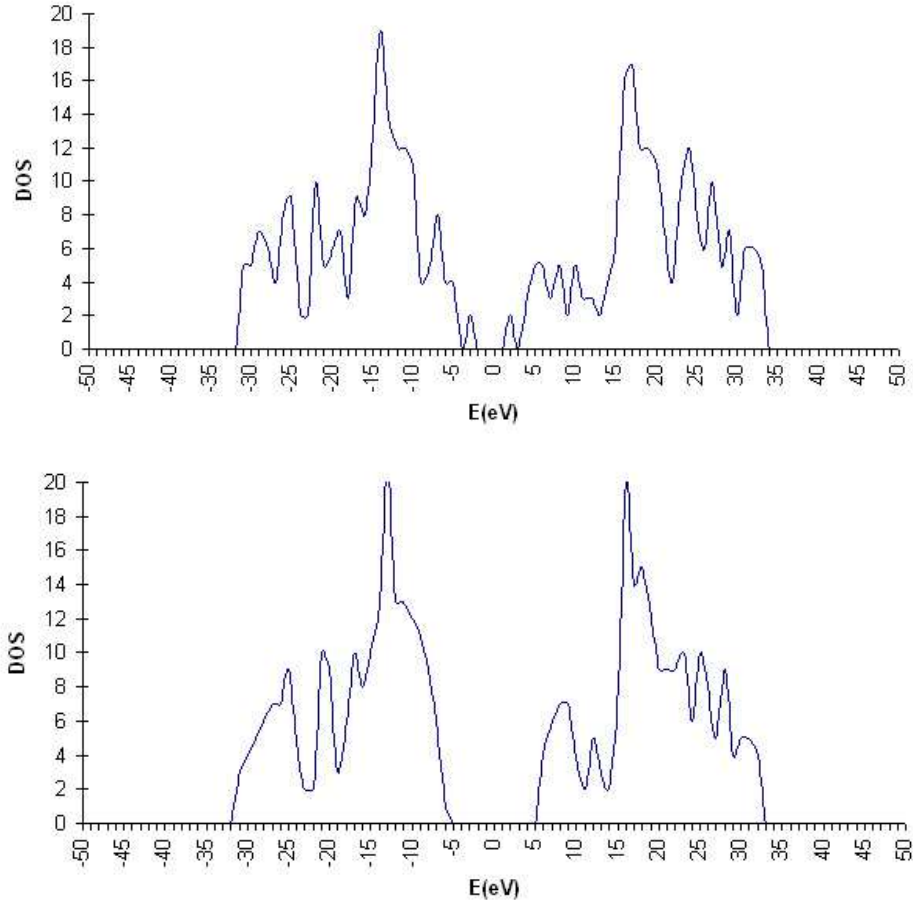


Fig. 4. (Color online.) Showing the DOS for pure coronene 37 (upper panel), and for coronene 37 with a chemisorbed H atom (lower panel), as a function of energy.

for coronene 37. We note that (i) a nearly straight line joins the peaks near the HOMO energy: such a trend mimics the linear dependence which is found in the DOS near the Fermi level in the infinite system [7]; (ii) particle-hole symmetry is absent, as is obtained in tight-binding calculations with a nonzero next-nearest hopping parameter  $t'$  [7]. However, here this asymmetry is not very pronounced than in the case  $t' \neq 0$ . This is probably due to the fact that in our calculations we do not restrict the interaction to next-nearest neighbors. We have also considered the level-spacing distribution  $P(s)$ , where the dimensionless spacing  $s$  is defined as the energy difference  $\Delta E_i = E_i - E_{i-1}$  between successive levels, divided by the average  $\langle \Delta E_i \rangle$  of the energy difference between successive levels [33]. The quantity  $P(s)$  yields the number of energy differences for which  $s - \Delta/2 < \Delta E_i / \langle \Delta E_i \rangle \leq s + \Delta/2$ , where  $\Delta$  is the step of the histogram. We have found that  $P(s)$  strongly depends on the energy range considered around  $E = 0$  (cf. Fig. 5). One can also recognize a strong dependence on the cluster size, so that no definite conclusion can be achieved at the present status of the calculations.

### 3.2 Clusters with a chemisorbed H atom

The largest cluster considered in the presence of a chemisorbed H atom is reported in Fig. 6, where the H adatom is depicted with a yellow color. The total energy, as a function of the cluster size and the approximation used, is quite similar to that reported in Fig. 2, and will not be shown here.

We find an average equilibrium distance of 1.53 Å between two in-plane nearest neighbor C atoms, forming an angle  $\angle\text{HCC}=105.3^\circ$  with the H adatom, while the C atom, on top of which the H atom resides, emerges from the plane of 0.71 Å. The distance of the H atom from the underneath C atom is 1.10 Å. The distance of the C atoms surrounding the adatom is of 0.30 Å with respect to the planar configuration. These values are in qualitative agreement with recent DFT calculations [34]. We find that (i) the most stable position is that with H on top of a carbon atom; (ii) the underlying C atom is induced out of the plane; (iii) there are small differences between the  $\alpha$  and  $\beta$  sets of eigenvalues positions. We will therefore report only the results for the  $\alpha$  set.

An important difference found in the presence of a chemisorbed H atom, with respect to the pure graphene clusters discussed in Sec. 3.1, is the trend of the gap as a function of the number of the benzene rings in the cluster, which is reported in Fig. 7. No evidence of a gap decrease appears in this case, which supports the results of Pereira *et al.* [17] that hydrogen chemisorption on graphene induces the opening of a gap. Also in agreement with such findings [17] is the behavior of the DOS, which is reported a dashed blue line in Fig. 4. One can see a clear enhancement of the DOS near the HOMO level, which Pereira *et al.* [17] have found as due to a resonance induced by the chemisorbed hydrogen. Of course, in this case we have used UHF calculations, which allowed us to estimate also the magnetic moment acquired by the H atom, which for a coronene 37 cluster is  $-0.33 \mu_B$ .

The above mentioned results, in the framework here considered, do not depend strongly on the cluster size considered, as reported in Tab. 1, where a comparison is presented between the results obtained with the coronene 19 and the coronene 37 clusters, by using a STO-3G basis set.

### 3.3 Clusters with a vacancy

In Fig. 8 we report the clusters considered in the presence of a vacancy. The same considerations made above for the total energy per number of benzene rings in Sec. 3.1 and 3.2 above apply to this case as well. The most stable electronic configuration is the triplet state, and the gap has a similar trend and similar values as those obtained for H chemisorption (cf. Tab. 1). From



Table 1

Showing values of the total energy  $E$  (Hartree), HOMO energy (Hartree), LUMO energy (Hartree), HOMO-LUMO gap (eV), and magnetic moment  $\mu$  ( $\mu_B$ ), for the coronene 19 and coronene 37 clusters, and the same clusters with a H adatom on top, with a vacancy, with substitutional proton, and with a substitutional H atom, using a STO-3G basis set.

	$E$	HOMO	LUMO	gap	$\mu$
coronene 19					
pure	-2030.796	-0.159	0.128	7.810	—
with H top	-2031.701	-0.252	0.243	13.465	-0.333
with vacancy	-1993.461	-0.262	0.216	13.007	1.838
with proton	-1993.834	-0.335	-0.120	5.850	0.917
with H subst.	-1994.058	-0.263	0.212	12.925	0.849
coronene 37					
pure	-3605.818	-0.137	0.101	6.476	—
with H top	-3607.059	-0.251	0.240	13.361	-0.334
with vacancy	-3568.808	-0.259	0.215	12.898	1.838
with proton	-3569.186	-0.319	-0.114	5.578	0.833
with H subst.	-3569.401	-0.261	0.212	12.871	0.851

Fig. 9, one can see that also in this case the DOS presents an increase near the HOMO level with respect to the case in the absence of the vacancy. The main difference with respect to the case with H on top, is relative to the magnetic moment acquired by a carbon atom near the vacancy (see atom labelled C<sup>68</sup> for coronene 37 in Fig. 8). The value obtained in this case is  $\approx 1.84 \mu_B$ , which presents just small changes in going from coronene 19 to coronene 37, or by using the  $\alpha$  or  $\beta$  sets of eigenvalues. The fact that the magnetic moment is smaller when we consider H chemisorption instead of a vacancy is in qualitative agreement with the results of Yaziev and Helm [35]. These authors have found  $1 \mu_B$  per hydrogen chemisorption defect, and  $1.12 - 1.53 \mu_B$  per vacancy defect, depending on the defect concentration. A value of  $1.52 \mu_B$  for a monovacancy is reported by Choi *et al.* [32]. From this comparison, we can deduce that the magnetic moments are sensitive to the model calculations employed, but our results are in overall agreement with the most recent works.

Fig. 10 and Tab. 2 report the distances between the various C atoms around the vacancy.

Table 2

Distances (in Å) between the various C atoms ( $i, j$ ) around the vacancy, as listed in Fig. 10.

$i$	$j$	$d_{ij}$
68	69	1.38
68	70	1.38
68	71	2.39
68	66	2.39
68	17	2.77
68	6	2.77
68	1	2.63
68	5	2.63
68	80	2.41
68	82	2.41

### 3.4 Clusters with a substitutional proton

Last, we have considered the same clusters as in Fig. 1, but now with a proton substituting a carbon atom at the cluster center. Such a configuration has been realized by considering a de-electronated hydrogen atom. The same considerations for the total energy apply also to this system, as discussed in the previous sections. The distances between the proton and the nearest neighbor C atoms are 1.03 Å for the C<sup>68</sup> atom, and 1.83 Å for the other two next nearest neighbor atoms. The cluster turns out to be flat. The DOS presents a peak near zero energy (cf. Fig. 9), as found by several authors when considering the effect of impurities in graphene [17,36]. We note that, for a substitutional proton, the gap is more than a half smaller with respect to the cases considered in Sections 3.2 and 3.3 (Cf. Tab. 1). It is even smaller with respect to a cluster with a substitutional H, *i.e.* a system presenting charge neutrality, which is also reported in Tab. 1. We argue that the gap is a sensitive quantity with respect to the injections of extra charges. The magnetic moment on the proton has an intermediate value with respect to the two cases considered previously. It is more sensitive to the cluster size going from 0.91  $\mu_B$  from coronene 19 to 0.83  $\mu_B$  for coronene 37, but is similar to that obtained for the substitutional H, which is 0.85  $\mu_B$  for both clusters (cf. Tab. 1). The present model is probably the most interesting in relation to the experiments performed by irradiating graphite with protons [9].

## 4 Conclusions

In the present work we have followed a ‘molecular’ approach to study impurity effects in graphene. The impurities considered were a chemisorbed H atom, a vacancy, and a positively charged substitutional H. We modelled these systems by considering clusters containing up to 37 benzene rings. We performed HF and UHF calculations using the STO-3G basis set.

The main emphasis of this work is not on correlation effects, which in some cases have been treated at the MP2 level, but on the size of the cluster. From the results discussed in the present work, we believe that coronene 37 is sufficiently large to ensure a local behavior similar to that of bulk graphene, especially near the center of the cluster. This is supported by the small changes in the physical properties studied here in going from coronene 19 to coronene 37. Of course, some features differ considerably from the finite clusters and the infinite system. For instance, we still observe quite a large gap in the density of states of finite clusters, as compared to that of graphene, while we have shown some important trends, which look quite promising in interpreting the general features of graphene: (i) The gap decreases by increasing the cluster size; (ii) The gap does not decrease if we consider H chemisorption or a vacancy; (iii) the gap is drastically reduced if we consider a substitutional proton. Other important features are: (i) an increase of the DOS near the HOMO level for all the impurities considered here with respect to the pure system; (ii) the appearance of a zero mode in the DOS if we consider a substitutional proton.

These results are for many aspects in agreement with the theoretical work of Pereira *et al.* [17], who have studied local disorder in graphene by using a tight-binding approach. Such a method allowed these authors to treat lattices with  $4 \times 10^6$  carbon atoms, thus reaching the size of real samples. However, they cannot treat lattice distortions around the defect, or the specific features connected with the particular impurity introduced.

In agreement with experiments [9], we have found that chemisorbed H, substitutional proton, and C atom near a vacancy acquire a magnetic moment. The determination of a precise value thereof is quite delicate, but we believe that the trend on going from one defect to another is correct, in view of the comparison of our results with the calculations of Yazyev and Helm [35].

We could not derive definite conclusions as regards the spacing of the levels near the HOMO state, and further work is thus required in this direction. In the future, it should be possible to treat even larger clusters, and these will be able to treat more realistically especially graphene quantum dots. We find that the gap strongly depends on the graphene cluster size, so that it is essential to control the size of graphene quantum dots in order to obtain a particular

gap value. This is relevant for the design of novel electronic devices, as well as it is important to control the impurity level.

## Acknowledgements

The authors thank Professor N. H. March for useful discussions over the general area embraced by the present paper.

## References

- [1] P. R. Wallace, *Phys. Rev.* **71**, 622 (1947).
- [2] C. A. Coulson and R. Taylor, *Proc. Phys. Soc. A* **65**, 815 (1952).
- [3] G. W. Semenoff, *Phys. Rev. Lett.* **53**, 2449 (1954).
- [4] K. S. Novoselov, A. K. Geim, S. V. Morozov, D. Jiang, Y. Zhang, S. V. Dubonos, I. V. Grigorieva, and A. A. Firsov, *Science* **306**, 666 (2004).
- [5] M. I. Katsnelson and K. S. Novoselov, *Solid State Commun.* **143**, 3 (2007).
- [6] Qimin Yan, Bing Huang, Jie Yu, Fawei Zheng, Ji Zang, Jian Wu, B.-L. Gu, Feng Liu, and Wenhui Duan, *Nanolett.* **7**, 1469 (2007).
- [7] A. H. Castro Neto, F. Guinea, N. M. R. Peres, K. S. Novoselov, and A. K. Geim, *Rev. Mod. Phys.* ..., ... (2008), [arXiv.org:0709.1163](https://arxiv.org/abs/0709.1163).
- [8] A. C. Dillon, K. M. Jones, T. A. Bekkedahl, C. H. Kiang, D. S. Bethune, and M. J. Heben, *Nature* **386**, 377 (1997).
- [9] P. Esquinazi, D. Spemann, R. Höhne, A. Setzer, K.-H. Han, and T. Butz, *Phys. Rev. Lett.* **91**, 227201 (2003).
- [10] L. Hornekær, E. Rauls, W. Xu, Ž. Šljivančanin, R. Otero, I. Stensgaard, E. Lægsgaard, B. Hammer, and F. Besenbacher, *Phys. Rev. Lett.* **97**, 186102 (2006).
- [11] V. V. Cheianov and V. I. Fal'ko, *Phys. Rev. Lett.* **97**, 226801 (2006).
- [12] K. H. Lau and W. Kohn, *Surf. Sci.* **75**, 69 (1978).
- [13] C. Bena, *Phys. Rev. Lett.* **100**, 076601 (2007).
- [14] P. Mallet, F. Varchon, C. Naud, L. Magaud, C. Berger, and J.-Y. Veuillen, *Phys. Rev. B* **76**, 041403(R) (2007).
- [15] P. Ruffieux, O. Gröning, P. Schwaller, L. Schlapbach, and P. Gröning, *Phys. Rev. Lett.* **84**, 4910 (2000).

- [16] P. Ruffieux, M. Melle-Franco, O. Gröning, M. Biemann, F. Zerbetto, and P. Gröning, *Phys. Rev. B* **71**, 153403 (2005).
- [17] V. M. Pereira, J. M. B. Lopes dos Santos, and A. H. Castro Neto, *Phys. Rev. B* **77**, 115109 (2008).
- [18] S. Klose, *Astron. Astrophys.* **260**, 321 (1992).
- [19] T. Fromherz, C. Mendoza, and F. Ruetter, *Mon. Not. R. Astron. Soc.* **263**, 851 (1993).
- [20] S. Patchkovskii, J. S. Tse, S. N. Yurchenko, L. Zhechkov, Th. Heine, and G. Seifert, *Proc. Nat. Acad. Sci. USA* **102**, 10439 (2005).
- [21] Ch. Møller and M. S. Plesset, *Phys. Rev.* **46**, 618 (1934).
- [22] J. Martin, N. Akerman, G. Ulbricht, T. Lohmann, J. H. Smet, K. von Klitzing, and A. Yacoby, *Nat. Phys.* **4**, 144 (2008).
- [23] F. Siringo, Ph.D. thesis, University of Catania, Italy, 1984.
- [24] The method employed was the same used by Piccitto *et al.* [37] for studying the correlation effects of chemisorbed H on transition metals surfaces, but the graphene band structure was calculated within the tight-binding approximation.
- [25] L. A. Ponomarenko, F. Schedin, M. I. Katsnelson, R. Yang, E. W. Hill, K. S. Novoselov, and A. K. Geim, *Science* **320**, 356 (2008).
- [26] M. J. Frisch, G. W. Trucks, H. B. Schlegel, G. E. Scuseria, M. A. Robb, J. R. Cheeseman, J. A. Montgomery, Jr., T. Vreven, K. N. Kudin, J. C. Burant, J. M. Millam, S. S. Iyengar, J. Tomasi, V. Barone, B. Mennucci, M. Cossi, G. Scalmani, N. Rega, G. A. Petersson, H. Nakatsuji, M. Hada, M. Ehara, K. Toyota, R. Fukuda, J. Hasegawa, M. Ishida, T. Nakajima, Y. Honda, O. Kitao, H. Nakai, M. Klene, X. Li, J. E. Knox, H. P. Hratchian, J. B. Cross, V. Bakken, C. Adamo, J. Jaramillo, R. Gomperts, R. E. Stratmann, O. Yazyev, A. J. Austin, R. Cammi, C. Pomelli, J. W. Ochterski, P. Y. Ayala, K. Morokuma, G. A. Voth, P. Salvador, J. J. Dannenberg, V. G. Zakrzewski, S. Dapprich, A. D. Daniels, M. C. Strain, O. Farkas, D. K. Malick, A. D. Rabuck, K. Raghavachari, J. B. Foresman, J. V. Ortiz, Q. Cui, A. G. Baboul, S. Clifford, J. Cioslowski, B. B. Stefanov, G. Liu, A. Liashenko, P. Piskorz, I. Komaromi, R. L. Martin, D. J. Fox, T. Keith, M. A. Al-Laham, C. Y. Peng, A. Nanayakkara, M. Challacombe, P. M. W. Gill, B. Johnson, W. Chen, M. W. Wong, C. Gonzalez, and J. A. Pople, *Gaussian 03, Revision C.02*, Gaussian, Inc., Wallingford, CT, 2004.
- [27] E. Stolyarova, K. T. Rim, S. Ryu, J. Maultzsch, P. Kim, L. E. Brus, T. F. Heinz, M. S. Hybertsen, and G. W. Flynn, *Proc. Nat. Acad. Sci.* **104**, 9209 (2007).
- [28] J.C. Meyer, A. K. Geim, M. I. Katsnelson, K. S. Novoselov, D. Obergfell, S. Roth, C. Girit, and A. Zettl, *Sol. State Commun.* **143**, 101 (2007).
- [29] R. E. Peierls, *Helv. Phys. Acta* **7**, 81 (1934).

- [30] N. D. Mermin and H. Wagner, Phys. Rev. Lett. **17**, 1133 (1966).
- [31] N. D. Mermin, Phys. Rev. **176**, 250 (1968).
- [32] S. Choi, B. W. Jeong, S. Kim, and G. Kim, ... ..., ... (2008), [arXiv.org:0805.2213](https://arxiv.org/abs/0805.2213).
- [33] H. De Raedt and M. I. Katsnelson, ... ..., ... (2008), [arXiv.org:0804.2758](https://arxiv.org/abs/0804.2758).
- [34] D. W. Boukhvalov, M. I. Katsnelson, and A. I. Lichtenstein, Phys. Rev. B **77**, 035427 (2008).
- [35] O. V. Yazyev and L. Helm, Phys. Rev. B **75**, 125408 (2007).
- [36] B. Y.-K. Hu, E. H. Hwang, and S. Das Sarma, ... ..., ... (2008), [arXiv.org:0805.2148](https://arxiv.org/abs/0805.2148).
- [37] G. Piccitto, F. Siringo, M. Baldo, and R. Pucci, Surf. Sci. **167**, 437 (1986).

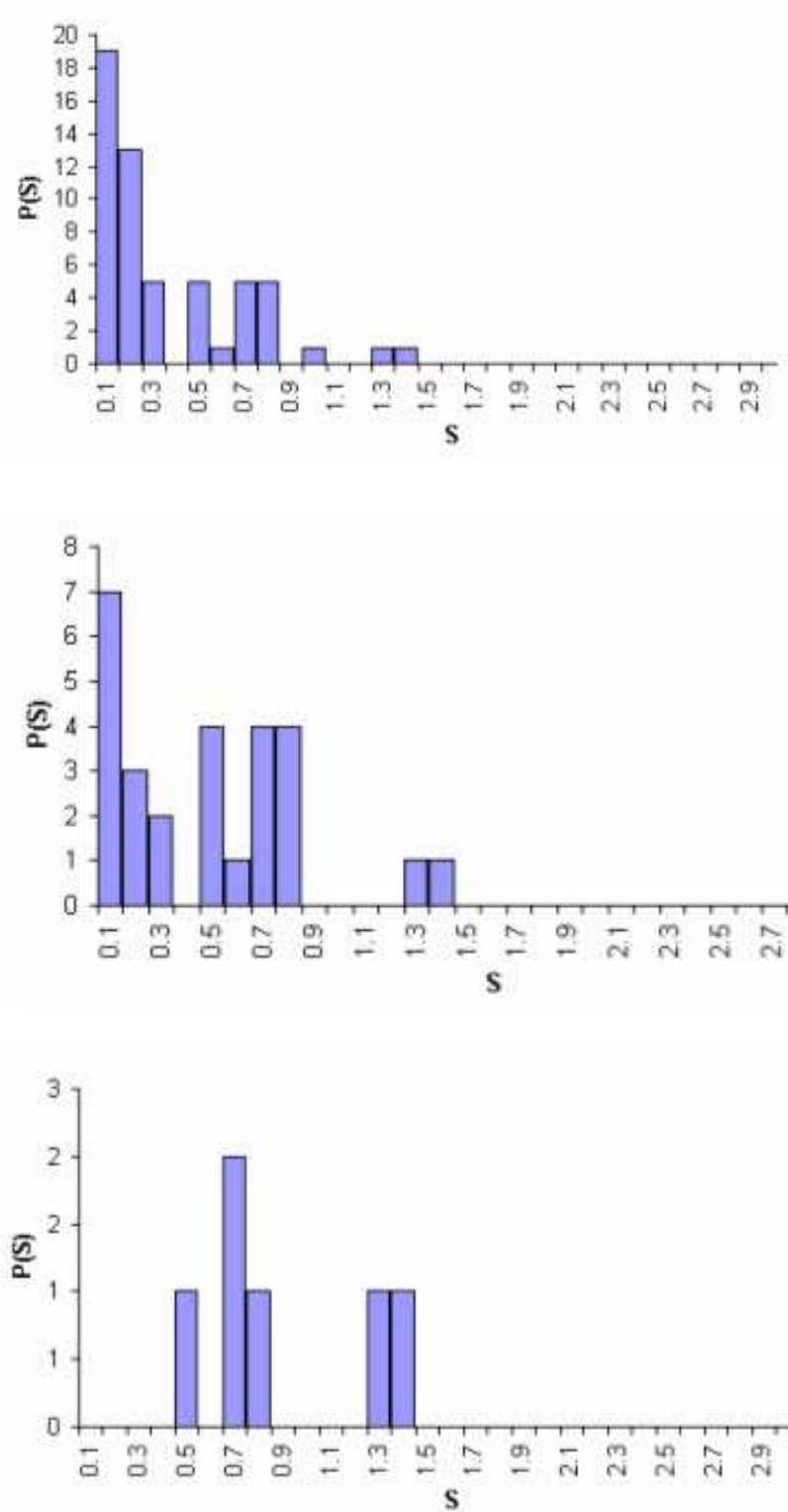


Fig. 5. (Color online.) Showing the level-spacing distribution  $P(s)$  for coronene 37, corresponding to different energy intervals centered around zero: 15 eV (topmost panel), 10 eV (intermediate panel), 5 eV (bottom panel). It can be noted that  $P(s)$  loses the Poissonian behavior in favor of a Gaussian behavior as the energy interval decreases.

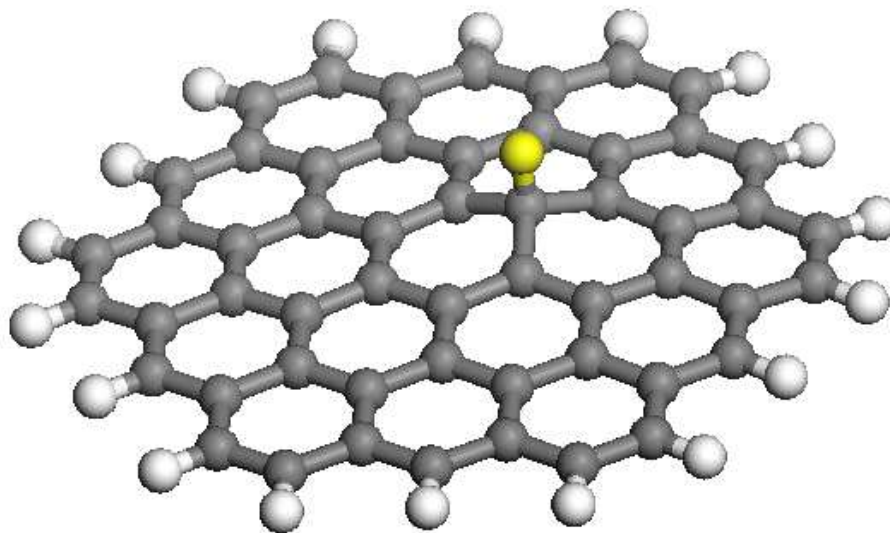


Fig. 6. (Color online.) Showing coronene 37 with a chemisorbed H atom.

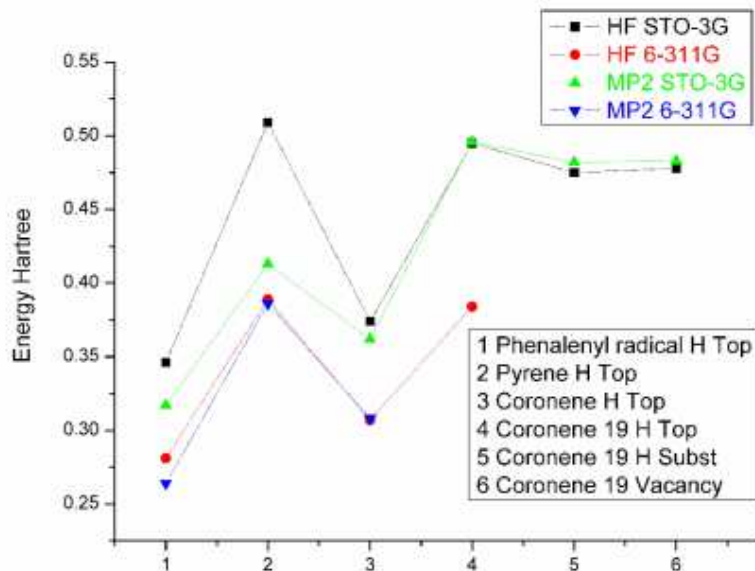


Fig. 7. (Color online.) Showing the dependence of the HOMO-LUMO difference (gap energy) *vs* the various clusters considered, in the presence of a chemisorbed H atom, for the different methods and basis sets employed in this work.



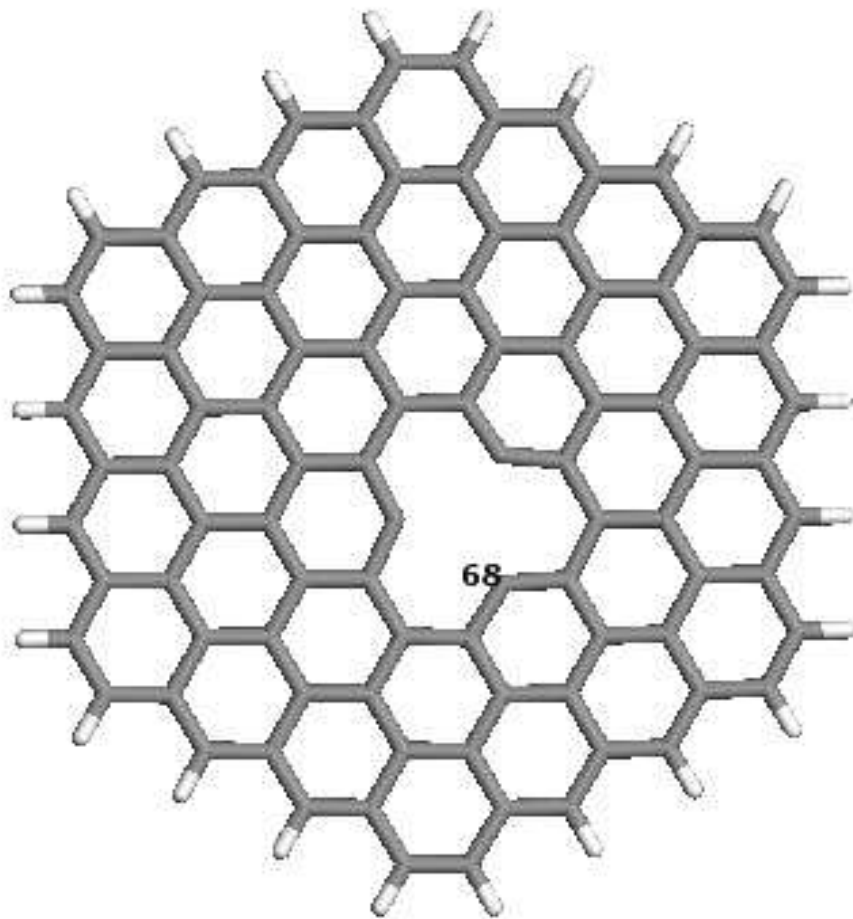


Fig. 8. (Color online.) Showing coronene 37 in the presence of a vacancy. Number 68 indicates the position of the C atom around the vacancy referred to in the main text.

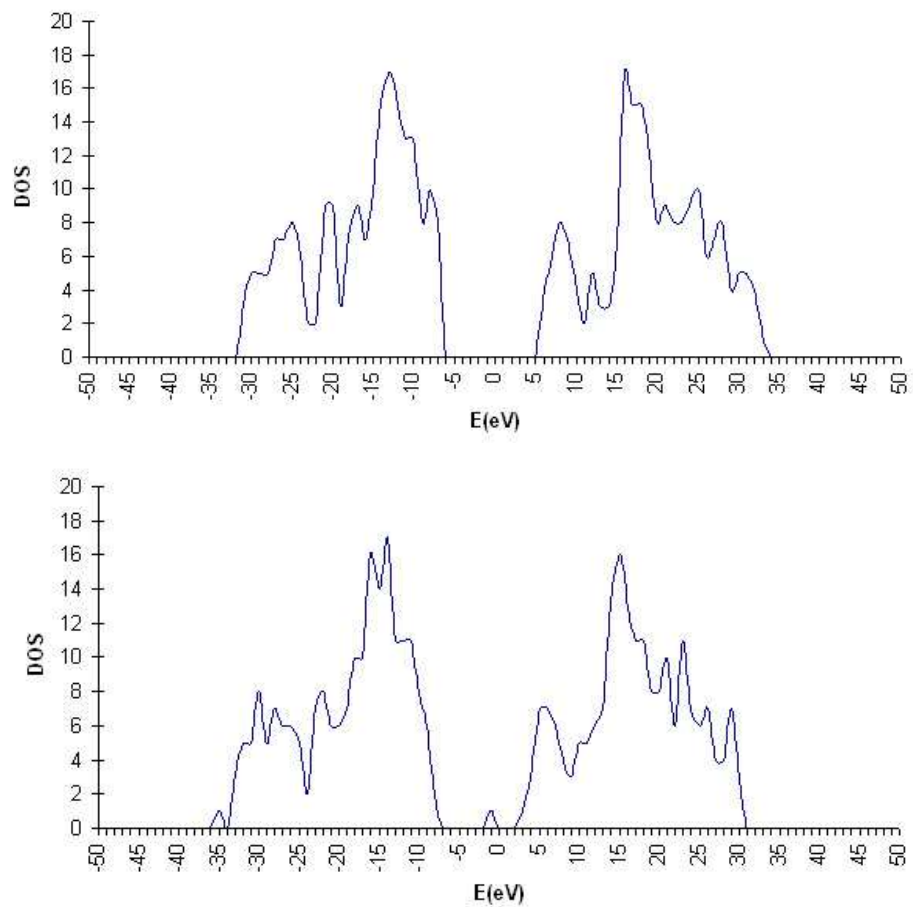


Fig. 9. Upper panel: Showing DOS of coronene 37 with a vacancy. Lower panel: Showing DOS of coronene 37 with a substitutional proton.

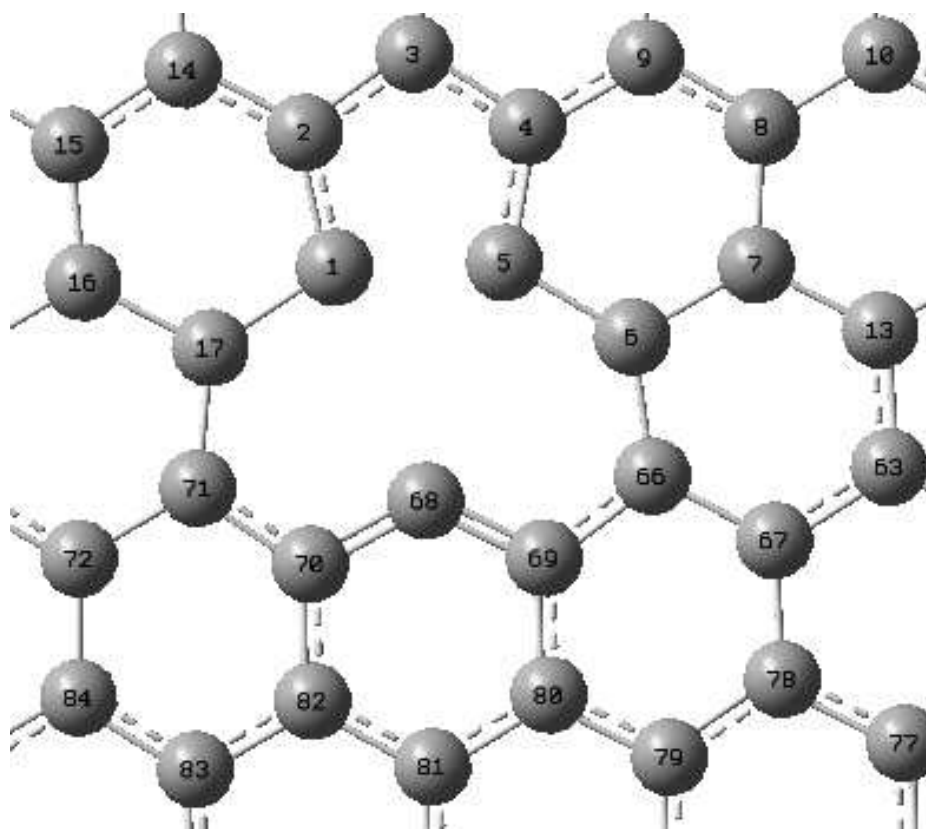


Fig. 10. Showing C atoms around the vacancy. The distances between the various atoms are reported in Tab. 2.